Proceedings World Geothermal Congress 2000
Kyushu - Tohoku, Japan, May 28 - June 10, 2000

DETERMINATION OF STRESS STATE AT THE HIJIORI HDR SITE FROM FOCAL MECHANISMS

Shunji Sasaki and Hideshi Kaieda

Central Research Institute of Electric Power Industry, 1646 Abiko, Abiko-city, Chiba 270-1194, Japan

Key word: stress inversion, microseismic event, induced seismicity, fault plane solution, regional stress state, HDR

ABSTRACT

The stress field around the Hijiori HDR geothermal energy site, Yamagata, Japan, was estimated by inverting the focal mechanism solutions of microseismic events induced during the various experiments. The stress inversion results show the maximum and intermediate principal stresses are in the direction inclining about 45° eastward and westward, respectively, from the vertical direction. The minimum principal stress orientation is nearly horizontal and trends north - south. The stress ratio indicates a value as small as 0.1. According to the results of the present study, the stress field in the Hijiori HDR site is in a state in which the maximum principal stress is almost equal to the intermediate principal stress.

1. INTRODUCTION

Since 1985, the New Energy and Industrial Technology Development Organization (NEDO) has been conducting research to develop elementary technologies for Hot Dry Rock (HDR) geothermal energy extraction at Hijiori, Yamagata Prefecture, Japan. The extraction of energy from HDR requires the creation of a man-made geothermal reservoir (fracture) between an injection well and a production well. This geothermal reservoir, which acts as a heat-exchange interface, is created artificially by hydraulic fracturing. Since propagation of hydraulically created fractures strongly depends on the regional stress state, it is necessary to clarify the stress state to create the man-made fractures.

For this purpose, the stress estimate at the Hijiori site has been investigated by using various methods such as differential strain curve analysis, the AE Kaiser effect observed during compression test of the core, etc. (Yamaguchi *et al*., 1996). On the other hand, hypocentral distributions of microseismic events associated with hydraulic fracturing experiments and circulation tests have been used as an efficient method to obtain information about the shape and propagation of hydraulically created fractures. Besides, determining the focal mechanism solutions of microseismic events makes it possible to evaluate the mechanism of a seismic event, as well as the direction of P and T axes, which approximately correspond to the maximum and minimum principal stresses.

We determine the focal mechanism solutions of microseismic events induced during various experiments conducted at the Hijiori HDR site, and try to find the stress field in the region based on the focal mechanism data. This study follows the basic approach of Gephart and Forsyth (1984).

2. OVERVIEW OF EXPERIMENTS

The outline of the experiments conducted by NEDO at the Hijiori HDR site is summarized as follows (Sato and Abé,1996).

2.1 Hydraulic fracturing experiment in 1988

A hydraulic fracturing experiment was carried out with SKG-2 (depth: 1802 m) as an injection well, and a 1800 m deep reservoir was created. In the hydraulic fracturing experiment, a total of about 2000 m^3 of water was injected from SKG-2 at four stages of flow rate, i.e., 1, 2, 4 and 6 m^3/min.

2.2 Circulation Test in 1989

A 30-day circulation test was conducted with SKG-2 as the injection well and HDR-1 (depth: 1805 m) and HDR-2 (depth: 1910 m) as production wells. In the 30-day circulation test, water was continuously injected into SKG-2 at the flow rate of 1 to 2 m^3/min, and steam and hot water were recovered from HDR-1 and HDR-2. The total amount of water injected during this test was about 44500 m^3 and the total production volume was about 13000 m^3.

2.3 Hydraulic Fracturing Experiment in 1992

After HDR-1 was deepened from 1805 m to 2205 m, a hydraulic fracturing experiment was carried out with HDR-1 as the injection well, and a 2200 m deep reservoir was created. In this experiment, a total of 2115 m^3 water was injected from HDR-1 at three stages of flow rate, i.e., 1, 2 and 4 m^3/min.

2.4 Circulation Test in 1995

With HDR-1 as the injection well and the deepened HDR-2 (depth: 2302 m) and the newly drilled HDR-3 (depth: 2302 m) as production wells, a 25-day circulation test was conducted. In the 25-day circulation test, water was continuously injected into HDR-1 at a flow rate of 1 to 2 m^3/min, and steam and hot water were recovered from HDR-2 and HDR-3. The total amount of water injected during this test was about 51500 m^3, and the amount of hot water and steam recovered was about 20600 m^3.

The outline of the experiments is summarized in Table 1.

3. SEISMIC NETWORK AND SEISMIC EVENT LOCATIONS

A seismic network consisting of 10 stations (ST-1 to ST-10) deployed in circle at a radius of 1.5 to 3 km was constructed (Sasaki, 1998). The locations of each seismic station are shown in Fig. 1, together with those of the SKG-2, HDR-1, HDR-2 and HDR-3 wells. Arrival times of P and S waves were used in a least squares method to find the locations of the microseismic events. The initial hypocenter was assumed to be at the bottom of the injection well and the initial origin time was determined from the first P arrival time and S-P time at station ST-8 by assuming Poisson's ratio of 0.25. A one-dimensional velocity model was used for the determination of the hypocenter. Epicentral distributions of microseismic events associated with experiments conducted at the Hijiori site are shown in Fig. 2.

4. STRESS INVERSION

4.1 Focal Mechanism Data

The best fit double couple focal mechanisms were determined using the grid search program FOCMEC of Snoke *et al.*, (1984). Microseismic events marked with solid circles in Fig.2 were used for focal mechanism analysis. Each focal mechanism was constrained by 7 or more P wave first motions. The amplitude ratios of S to P recorded on vertical component seismographs were also used besides the P-wave first motions to constrain the range of possible solutions (Kisslinger, 1980). A total of 113 focal mechanism solutions were obtained. A number of solutions in each experiment was 15, 42, 15 and 42 in the 1988 hydraulic fracturing experiment, the 1989 circulation test, the 1992 hydraulic fracturing experiment and the 1995 circulation test, respectively. Examples of focal mechanism solutions obtained are shown in Fig. 3.

4.2 Stress Inversion Method

Several inverse techniques have been devised for finding the stress field, which is the most consistent with a heterogeneous set of focal mechanism data. In the following, the stress field around the Hijiori test site was determined using the focal mechanism stress inversion method of Gephart and Forsyth (1984). The objective of this method is to find the set of stress tensor that is most nearly consistent with all the observed focal mechanism data. The inversion scheme determines the orientation of three principal stress axes and the stress ratio (R) by minimizing the misfit angle between the direction of the predicted shear stress on the fault plane and the observed slip direction on each plane determined from focal mechanisms. The stress ratio measures the relative magnitude of three principal stresses, the maximum principal stress (σ_1), intermediate principal stress (σ_2), and, minimum principal stress (σ_3), using equation (1):

$$R = \frac{\sigma_2 - \sigma_1}{\sigma_3 - \sigma_1} \qquad (1)$$

The stress ratio varies from 0 to 1. When σ_2 and σ_3 are nearly equivalent, the stress ratio approaches 1, and when σ_2 and σ_1 are nearly equivalent, the stress ratio approaches 0. In implementing the grid search, σ_1 is first fixed, and a misfit measure is calculated for a range of R and for consistent values of σ_3 and σ_2 which satisfy the orthogonal condition. The process is progressively repeated using new trial values of σ_1 selected from a regular grid superimposed on an equal area projection. Misfits for each sampled value of the solution space (σ_1, σ_2, σ_3, R) are tabulated, and misfit based confidence limits over which solutions are not statistically different from the best solution are determined using one-norm statistics.

4.3 Results

The distributions of P and T axes of the focal mechanism solutions are shown in Figs. 4(1) to 4(4). P axes obtained from the focal mechanism solutions of microseismic events induced during the hydraulic fracturing experiments in 1988 and 1992 are distributed from almost vertical to the east and from vertical to the south, respectively. On the other hand, P axes obtained from the focal mechanism solutions of microseismic events associated with the circulation tests in 1989 and 1995 are distributed in all directions. The distributions of the P and T axes scatter largely in this manner, and it is generally difficult to determine the principal stress directions from the focal mechanism data.

<u>Stress inversion results from each focal mechanism data set</u>

The results obtained using the method of Gephart and Forsyth (1984) are shown in Figs. 5(1) to 5(4). These figures are the stress inversion results for the data set of focal mechanism solutions shown in Figs. 4(1) to (4) and show 95% confidence limits for the directions of maximum (circles), intermediate (squares) and minimum principal stress (triangles). The results shown in these figures may be summarized as follows. The stress inversion results obtained from the 1988, 1989 and 1995 focal mechanism data are similar to each other, that is, the maximum and intermediate principal stresses are in the direction inclining about 30° to 45° eastward and westward, respectively, from the vertical direction. The minimum principal stress is horizontal and is almost in the north-south direction. On the other hand, the results for the 1992 experiment show the maximum and intermediate principal stresses are in the direction inclining about 60° to 70° southward and eastward, respectively, from the vertical direction. Thus, the stress inversion results obtained from the 1992 focal mechanism data are different from those obtained from the 1988, 1989 and 1995 focal mechanism data. Its cause is not known at the present, so a further study will be made on this problem.

<u>Stress inversion results obtained using the combined use of data sets</u>

As mentioned above, the stress inversion results obtained from the 1992 focal mechanism data are different from those obtained from the 1988, 1989 and 1995 focal mechanism data. In the following, therefore, the stress inversion was implemented using all data sets excluding the 1992 data set. The stress inversion results are shown in Figs. 6(1) to (2). Fig. 6(1) shows the 95% confidence limits for the directions of the principal stress. Fig. 6(2) shows the stress ratio (equation (1)) corresponding to solutions within the maximum principal stress 95% confidence limits. The results obtained show the maximum principal stress and intermediate principal stress are in the direction inclining about 45° eastward and westward, respectively, from the vertical direction. The minimum principal stress is horizontal and is almost in the north-south direction. The stress ratio R shown in Fig. 6(2) indicates a value as small as 0.1. As is clear from equation (1), R = 0 holds when $\sigma_1 = \sigma_2$. According to the results of the present analysis, it can be said that the stress field around the Hijiori HDR site is in a state in which the maximum principal stress is almost equal to the intermediate principal stress.

Many researchers independently have attempted to determine the stress field in the Hijiori HDR site using such as the differential strain curve analysis method, the AE Kaiser effect test, the method based on a comparison between the dablet distribution plane and the mechanism solutions (Tezuka and Niitsuma, 1997). According to the results reviewed by Yamaguchi *et al*., (1996), the maximum principal stress is in the vertical direction while the minimum principal stress is in the north-south direction. Our result in general agrees with previous estimates of stress directions.

CONCLUSION

The stress field around the Hijiori area was determined by inverting the focal mechanism solutions of microseismic events induced during the hydraulic fracturing experiments and circulation tests. The stress inversion results show the maximum and intermediate principal stresses are in the direction inclining about 45° eastward and westward, respectively, from the vertical direction. The minimum principal stress orientation is nearly horizontal and trends north - south. The stress ratio indicates a value as small as 0.1. Our result in general agrees with previous estimates of stress directions.

ACKNOWLEDGEMENT

We would like to thank M. Fehler, Los Alamos National Laboratory, for providing valuable advice and computer code relating to the stress inversion problem. We are especially grateful to S. Sato, Yoshizawa Giken Inc. for his assistance. This research was conducted under contract with the New Energy and Industrial Technology Development Organization (NEDO) in FY 1997 and 1998.

REFERENCES

Gephart, J., and Horsyth, W. (1984). An improved method for determining the regional stress tensor using earthquake focal mechanism data: Application to the San Fernando earthquake sequence, J. Geophys. Res, 89, pp9305-9320.

Kisslinger, C. (1980). Evaluation of S to P amplitude ratios for determining focal mechanisms from regional network observations, Bull. Seism. Soc. Am, 70, pp999-1014.

Sasaki, S. (1998). Characteristics of microseismic events induced during hydraulic fracturing experiments at the Hijiori hot dry rock geothermal energy site, Yamagata, Japan, Tectonophysics, 289, pp171-188.

Sato, Y., and Abé, H. (1996). Review of procedures of HDR reservoir creation at Hijiori from design methodology, 3rd International HDR Forum, May 13-16, Santa Fe, New Mexico, USA, pp7-9.

Snoke, J. A., Munsey, J. W., Teague. A. G., and Bollinger, G. A. (1984). A program for focal mechanism determination by combined use of polarity and SV-P amplitude ratio data, Earthquake Notes, 55, No.3, P15.

Tezuka, K., and Niitsuma, H. Integrated interpretation of microseismic clusters and fracture system in a Hot Dry Rock artificial reservoir, SEG Expanded Abstracts, 657-660, 1997.

Yamaguchi, T., Oikawa, Y., Matsunaga, I., and Sato, Y. (1996). Estimation of in-situ stress state at Hijiori test site, 3rd International HDR Forum, May 13-16, Santa Fe, New Mexico, USA, pp13-14.

Table 1. Outline of experiments at the Hijiori HDR site

	type of experiment	jnjection well	injection interval (m)	maximum of flow rate (m^3/min)	total injection volume (m^3)	No. of fault plane solution
1988	hydrofracturing	SKG-2	1788-1802	6	1,961	15
1989	circulation	SKG-2	1788-1802	2	45,921	42
1992	hydrofracturing	HDR-1	2151-2205	4	2,115	15
1995	circulation	HDR-1	2151-2205	4	51,500	41

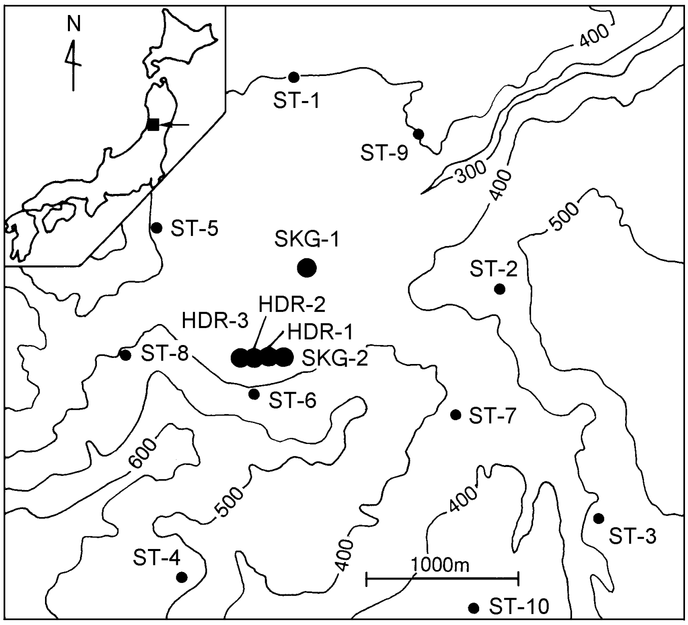

Fig.1. Locations of SKG-2, HDR-1, HDR-2 and HDR-3 wells at the Hijiori HDR site. ST-1 to ST10 (solid circles) are borehole seismic stations.

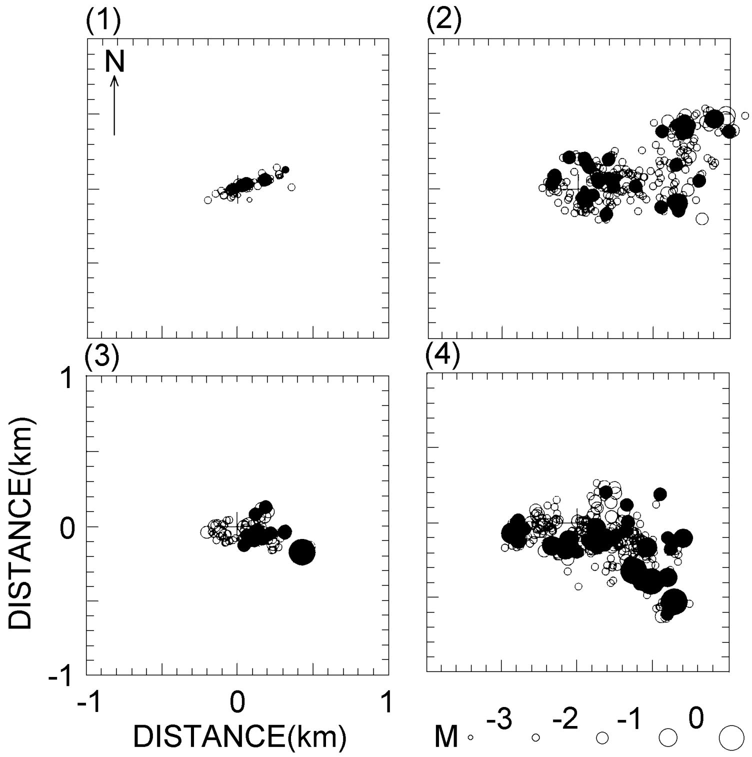

Fig.2. Epicentral distributions of microseismic events associated with (1) the 1988 hydraulic fracturing experiment, (2) the 1989 circulation test, (3) the 1992 hydraulic fracturing experiment, and (4) the 1995 circulation test, respectively. Symbols are proportional to size of microseismic events.

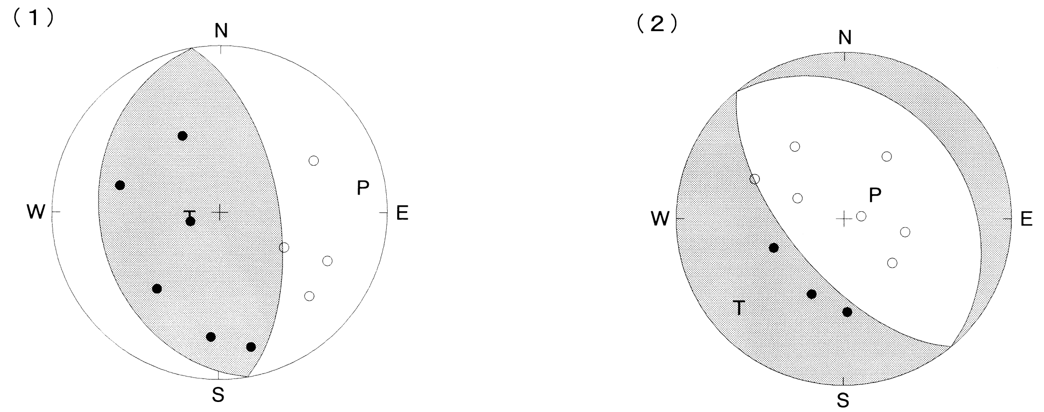

Fig.3. Examples of focal mechanism solutions of microseismic events. The diagram is an equal area projection of the lower hemisphere of the focal sphere. Open circles represent dilatational first motions, solid circles represent compressions. Symbols P, T are the P and T axes, respectively. Microseismic events with M=0.4 (top) and M=-0.5 (bottom) occurred during the 1995 circulation test.

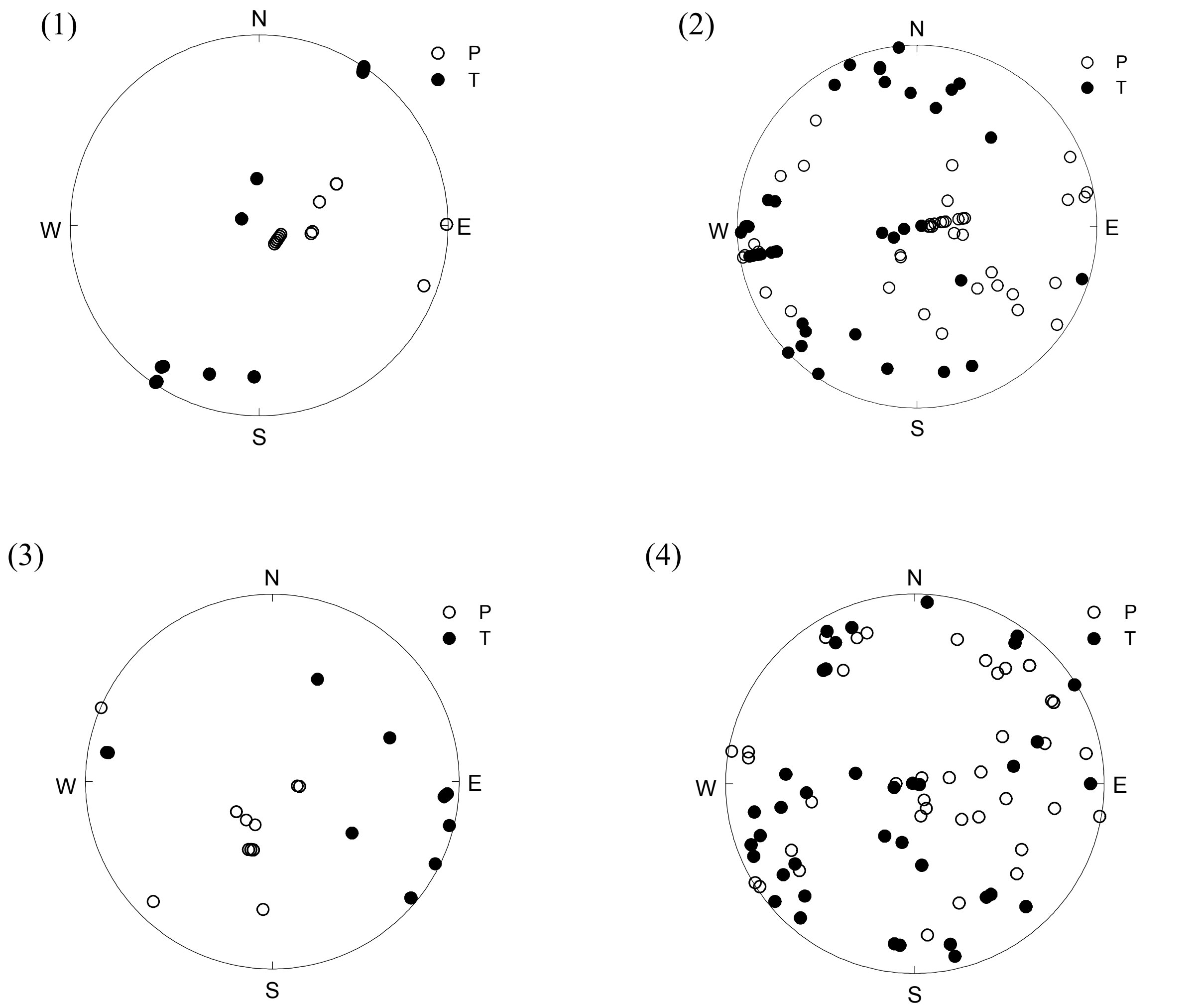

Fig.4. Equal area plots showing orientations of P axes (open circle) and T axes (solid circle) from focal mechanism solutions of microseismic events associated with (1) the 1988 hydraulic fracturing experiment, (2) the 1989 circulation test, (3) the 1992 hydraulic fracturing experiment, and (4) the 1995 circulation test, respectively.

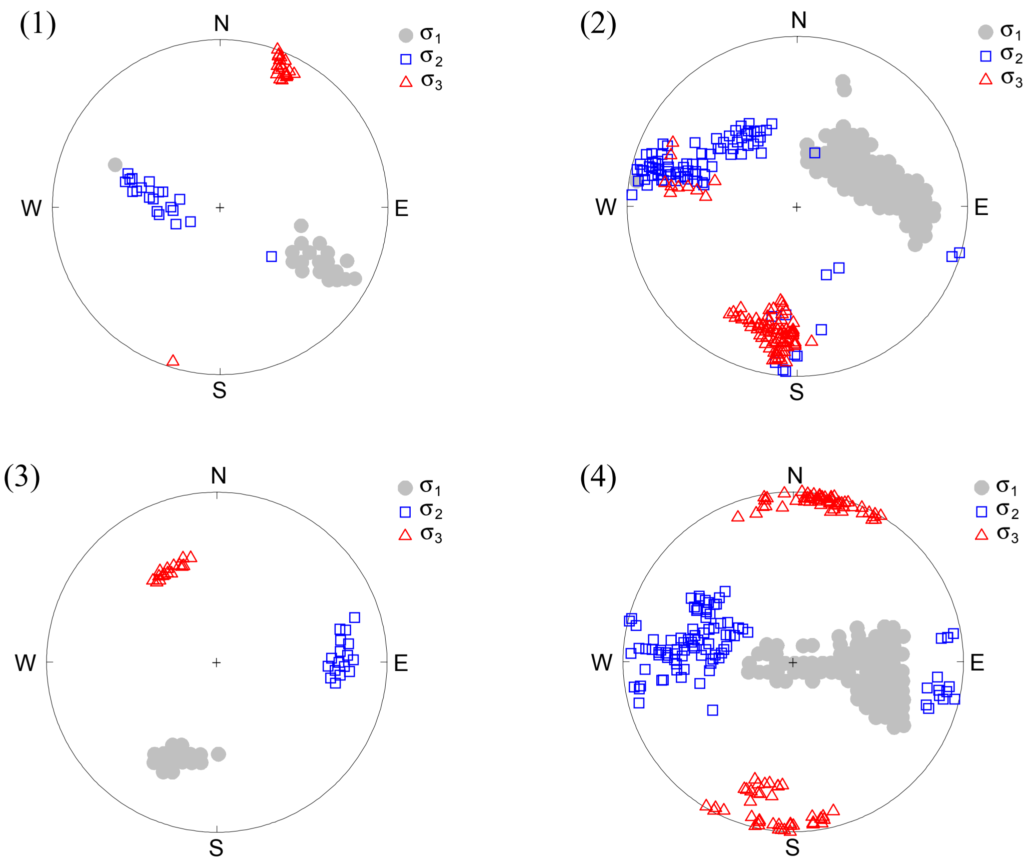

Fig. 5. Stress inversion results (equal area, lower hemisphere projection) showing orientations of σ_1(circles), σ_2(squares), and σ_3(triangles) of the stress models within the 95 % confidence limit of our analysis. (1) in case of the 1988 hydraulic fracturing experiment, (2) the 1989 circulation test, (3) the 1992 hydraulic fracturing experiment, and (4) the 1995 circulation test, respectively.

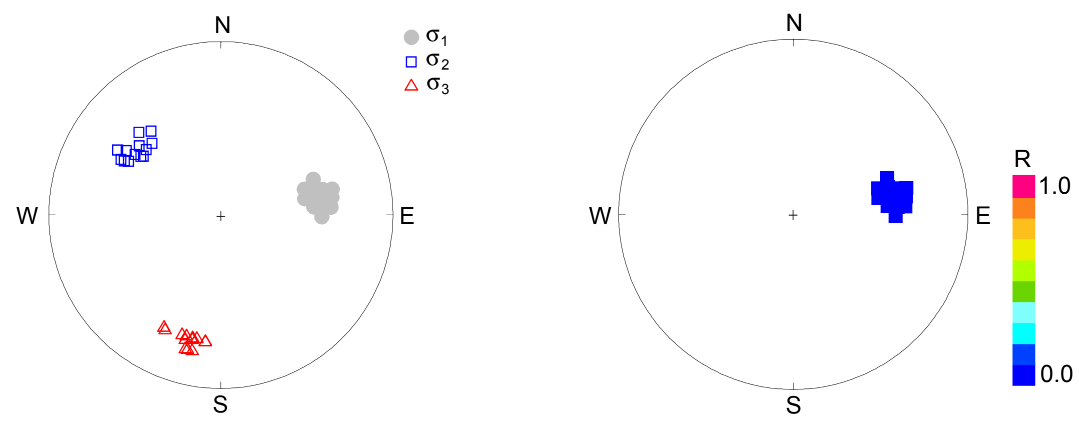

Fig.6. Stress inversion results obtained from combined use of the 1988, 1989 and 1995 focal mechanism data. (1) Orientations of σ_1(circles), σ_2(squares), and σ_3(triangles) of the stress models within the 95 % confidence limit (equal area, lower hemisphere projection). (2) Stress ratio corresponding to solutions within σ_1 95 % confidence limits.